Chapter 4

Integrated Scenario Modeling

4.1 Introduction and Overview of Integrated Scenario Modeling

Modeling of both experimentally achieved and projected future discharges is a critical component to NSTX's long term plan. Understanding the interactions of plasma transport, macroscopic stability, heating and current drive sources, and plasma edge effects in past experiments, and then being able to project these behaviors to design future experiments is a primary theme for the next five years.

Integrated scenario modeling of future NSTX performance serves at least three major functions:

1. It identifies ranges of experimental approaches that can be used to meet specific research goals, optimizing the use of valuable experimental run time.

2. It clarifies requirements for tools that need to be implemented to ensure success achieving the NSTX mission. These tools include those that will support development of the scientific basis for making sound extrapolations of ST performance.

3. Ultimately, integrated scenario modeling provides the framework for testing theoretical models enabling predictions to be made based on them and to be compared to experimental results.

This chapter focuses on the first two of these three elements.

Attractive operating scenarios have been identified as follows:

- Steady-state operations with HHFW and EBW in the 800kA range of operations with beta of 15% are credible targets for NSTX research. Neutral beam injection can also be used, but this is calculated to be at the expense of HHFW current drive efficiency. Such experiments will provide a well-controlled environment for developing and validating these current drive tools.
- Plasma regimes in the beta range of 46% can be reached energetically and with respect to macrostability of ideal modes, using inductive current drive. This will allow the study of much of the key stability, transport, and boundary physics that will be needed for the long-pulse non-inductive high beta operation, and will create a laboratory for the study of the new physics that may be manifest in plasmas with beta's of order unity.
- After plasma initiation by coaxial helicity injection or poloidal field induction, non-solenoidal current ramp to high poloidal beta plasmas is shown to be possible with a combination of HHFW heating, HHFW current drive, and bootstrap current. This is an important ingredient for confidence in the design of future ST devices.
- NSTX operating scenarios at high beta, high bootstrap current fraction, near the with-wall stability limit, without flux from the solenoid during the current flattop and for pulse lengths compared to a current relaxation time are calculated to be achievable with the plasma control tools described in this plan document, including a mix of neutral beam heating and current drive, HHFW heating, and EBW heating and current drive.

The tools required to implement these scenarios have been identified. Key elements include the following;

- EBW, through the Ohkawa effect, is ideally suited to take advantage of the high trapping fraction present in the ST magnetic geometry. It enables current drive efficiencies that are comparable to

or higher than those found with electron cyclotron current drive systems used on tokamaks, extendable to the far plasma periphery (Chapter 3.4).

- The flexibility of the off-axis current drive strategy offered by an Electron Bernstein Wave system provides the opportunity to achieve long pulse, fully non-inductive high beta operations. Off-axis currents theoretically achievable with 3 MW of EBW maintained elevated central q values needed for core second-stability to ballooning modes as well as for avoiding sawteeth.

- The EBW current density is predicted to exceed the local bootstrap current density in high beta NSTX plasmas and to be highly localized, providing a tool for neoclassical tearing mode suppression.

- EBW will provide a flexible tool for exploring and potentially modifying transport in the electron thermal channel (Chapter 3.2). Facility and development issues related to EBW development are described in Chapters 2, 3.2, and 3.4.

• The potential of HHFW for current drive in the presence of high ion temperature and energetic beam ions will continue to be explored vigorously, particularly at high beta, but the primary application of HHFW is most likey to be for heating in many scenarios, and for current drive in solenoid-free current ramp and sustainment experiments without strong ion heating.

• Density control, obtained through pumping and pellet injection, will be of substantial benefit for enabling flexibility in optimizing the beam driven current, and for enhancing the current drive efficiency for any implemented RF system. It can provide an important tool for modification of the plasma pressure profile and bootstrap current profile to optimize performance as well. This has prompted the NSTX program to propose a particle control strategy that includes both cryopumping and also the development of lithium-based particle handling technologies. The latter is a less well developed technology, but it has been shown on both TFTR and CDX-U to reduce recycling dramatically, with potentially very large impacts on profiles, and may lead to a liquid lithium divertor technology that will have broad impact for the future of the ST configuration and for all toroidal confinement concepts. These plan elements are discussed in Chapters 2 and 3.5.

- Modest modifications of the poloidal field coil system can have dramatic impacts on the available scenarios. Technical aspects of these modifications are described in Chapters 2 and 3.4 of the plan. In particular,
  - Splitting of poloidal field coil PF1A will allow operation with simultaneous high kappa and high delta, with the plasma edge closely contoured to the existing passive plates for optimized stability and control.
  - Energizing of an existing additional PF coil will also permit solenoid-free startup research using only external PF coils. This is a promising new avenue of research with potential applicability to advanced tokamak power plant designs as well.

4.2 Specific Goals of Integrated Scenario Modeling

The spherical torus concept will provide an attractive fusion energy configuration if it can demonstrate the following major features: high plasma elongation with significant triangularity, 100% non-inductive current with a credible path to high bootstrap current fractions, non-solenoidal startup/rampup of the plasma current, high β with stabilization of the RWM instabilities, and sufficiently high energy confinement. Demonstrating these features experimentally would certainly be achieved individually, and then simultaneously to varying degrees. Integrated scenario modeling is a key element to guide experiments toward achieving these features.

The long term planning for NSTX integrated scenario modeling involves a sequence of goals aligned with the experimental milestones. These include the following, which have a number of questions to be answered by simulations and experiments as they proceed;

- <u>100% non-inductive discharges for $t_{flattop} > \tau_{skin}$, utilizing NBI, HHFW and EBW CD</u>
  - What plasma parameters maximize HHFW and EBW CD contributions and how do the theory and experiment compare?
  - How will NBI contribute?
  - What are the benefits of plasma elongation and triangularity?

- What are β_N and HH requirements?
- What are the quasi-stationary current profiles?
- What is the ideal MHD stable operating regime?

- Maximum $\beta \geq 40\%$ and $\beta_N \geq 8$ for $t_{flattop} > \tau_E$

  - What are maximum β and β_N that can be sustained and at what (I_P, B_T) are these obtained?
  - How is RWM stabilization contributing to these β's?
  - Can confinement improvements be sustained?
  - What are plasma shapes that maximize β headroom?
  - What is the inductive current evolution and how can we optimize future non-inductive scenarios?

- Non-solenoidal rampup

  - What is the vertical field contribution during current rampup by heating and current drive?
  - What are the time-scales for current rampup?
  - What type of plasmas are produced in these low current and high pressure configurations, and what is their ideal MHD stability?

- Integration: 100% non-inductive, $\beta \geq 40\%$ and $\beta_N \geq 8$, for $t_{flattop} >> \tau_{skin}$, while maximizing f_{bs}

  - What are the best (I_p, B_T) combinations and how can this be expanded?
  - Do we need RWM stabilization by rotation and/or active feedback and what is its sustainability?
  - What are the quasi-stationary current profiles with 100% non-inductive current and large bootstrap current fraction?
  - What is the resulting bootstrap current profile?
  - What contributions from HHFW, EBW and NBI heating/CD are obtained/required?
  - What are the benefits of plasma shaping?

Predictive simulations were done with the Tokamak Simulation Code (TSC) to find ways to produce these plasmas based on existing experimental data and self-consistent integrated modeling. In addition,

extensive analysis with a stand-alone version of CURRAY will be shown to identify the best discharge parameters to maximize the HHFW current drive efficiency for the simulations where it is employed.

4.3 The Computational Tools and Experimental Coupling

The time-dependent computer codes used for integrated modeling are TRANSP and TSC (Tokamak Simulation Code). The former provides fixed-boundary evolutions, while the latter provides free-boundary evolutions. TRANSP is typically used as interpretive, such that it uses the experimental temperature and density profiles, and plasma boundaries to guide its simulations. A predictive capability is now available. TSC is predictive, although it contains modes where it is constrained by experimental data, such as line average density, PF coil currents, etc. Although the two codes are solving the same basic transport equations for energy and current density (and particles if chosen) using equilibrium flux geometry, they have different capabilities in terms of heating and CD calculations, models for transport coefficients, impurity treatment, sawtooth treatment, plasma rotation, bootstrap current, radiation, fast particle treatment, MHD stability, neutral particles, and plasma feedback models. These capabilities are continuously being expanded and updated.

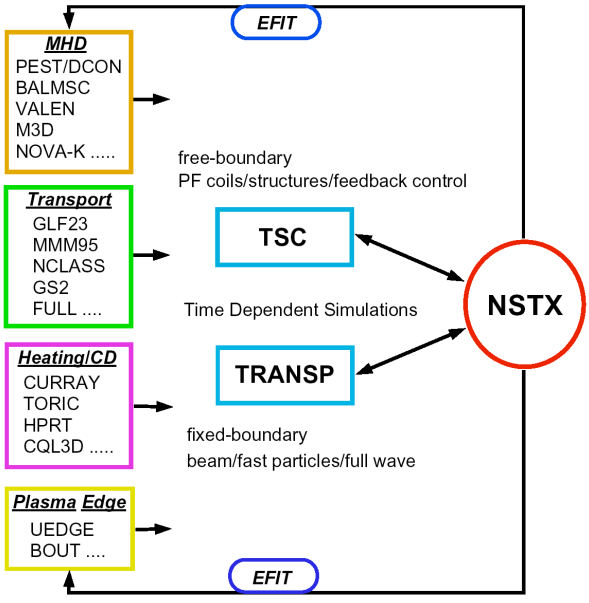

Figure 1. Schematic of integrated scenario modeling for NSTX, identifying the stand-lone simulations, time-dependent simulation, and experimental contributions and interactions

Although it is desirable to have integrated modeling with all physics models available, such a computer code does not yet exist, and so stand-alone analysis is important to supplement the evolution simulations with TRANSP and TSC. These stand-alone simulations typically rely on a static equilibrium at a given time slice and have no time dependent features. Since one is examining only a single time slice more sophisticated

computations can be done, as opposed to integrating it into a transport code that would have to do the computations a large number of times. Examples of the most commonly used analyses are CURRAY (HHFW), AORSA(HHFW), HPRT(HHFW), TORIC (HHFW), TRANSP (Monte Carlo NB), EIGOL(NB), VALEN (RWM), PEST/DCON/BALMSC (ideal MHD), CQL3D (RF), FULL (ITG/TEM), GS2 (ITG/ETG), M3D (resistive MHD), NOVA-K (fast particle instabilities) and there are several others. It should be noted, that some of these models are incorporated into TRANSP and TSC, and others will continue to be as computational capability expands. In addition, the equilibrium analysis with EFIT provides the experimental information for virtually all these stand-alone analyses, as well as guidance for both TRANSP and TSC.

Schematically shown in Fig. 1 is the interdependence of the stand-alone analysis, time dependent scenario modeling and experimental results. The stand-alone analysis feeds into integrated scenario modeling where it can not be included explicitly. TSC's primary strength which TRANSP can not include is its free-boundary plasma feature including interactions with the structure and PF coils, and feedback control systems. Presently TRANSP's particular strengths are the sophisticated physics models that can be included, especially the Monte Carlo beam deposition and fast particle treatment as well as its close coupling to experimental data. It should be noted that analysis with TSC and TRANSP are complementary, in particular, when interpretive TRANSP provides experimental thermal diffusivities and beam heating profiles for TSC simulations.

The scenario modeling is intimately coupled to experimental results, and relies on continuous advancement of physics models and computational capabilities. The experimental constraints are particularly evident in energy and particle transport since fully reliable predictive models, especially for low aspect ratios, do not exist. However, even in areas that are considered more mature, such as RF, experimental verification of heating/CD predictions is still critical due to complex damping dependences on plasma properties, presence of fast particles, and equilibrium geometry.

Since all the time-dependent scenario simulations presented here are being done with the Tokamak Simulation Code (TSC), a description of its physics modeling follows. TSC is a two-dimensional time-dependent free boundary simulation code that advances the MHD equations describing the transport time-scale evolution of an axisymmetric magnetized tokamak plasma. TSC evolves the magnetic field in a rectangular computational domain using the Maxwell-MHD equations for the plasma and passive

structures, coupled through boundary conditions to the circuit equations for the poloidal field coils. The plasma model in TSC is completed by providing functional forms for the electron and ion thermal diffusivities, for the particle diffusion and convection coefficients, and for the plasma electrical resistivity. Therefore, TSC solves 2D variables for the poloidal magnetic flux and toroidal field, but utilizes flux coordinate mappings to solve 1D equations for surface averaged temperatures and densities. The model includes separate energy and particle equations for electrons and ions, neoclassical resistivity, bootstrap current, various sawtooth models, various theory based models for energy and particle transport, radiation from impurities, various external non-inductive current sources, and ballooning stability. Due to its free-boundary treatment, TSC must be run with feedback systems operating which includes the interactions between PF coils and structures.

For the simulations shown here with TSC, the following prescriptions are used:

1) The density profile and magnitude is prescribed as a function of time.

2) The thermal diffusivities are taken from a TRANSP analysis of a discharge, 109070, and they are uniformly scaled according to IPB98(y,2) global energy confinement scaling.

3) The beam heating profile is taken from TRANSP, with beam driven current calculated in TSC (which was benchmarked against the TRANSP result). Beam characteristics (beam stored energy, fast ion density, and deposition profile) are fixed to those of shot 109070, and scaled by the injected power.

4) The Z_{eff} profile is taken from the experiment, having a hollow profile with a value of 2.5 at the plasma center and slightly over 4 at an r/a of 0.75.

5) A benchmark discharge simulation is done with TSC of 109070 in order to match several parameters before proceeding with extrapolations.

6) The HHFW only scenarios utilize the thermal diffusivities and prescribed density profile based on shots 106194 and 108901, and are scaled by an L-mode global energy confinement scaling, proportional to $Ip^{1.0}Bt^{-0.2}n^{0.6}P^{-0.6}$.

The CURRAY code will be used extensively to examine HHFW current drive under various situations in the scenarios. CURRAY is a 3D ray-tracing code for RF waves ranging in frequency from ion cyclotron to lower hybrid. It runs in toroidal geometry. The ray equations are based on the cold dispersion relation, with relevant thermal electron corrections. Solution of the ray equations provides the ray trajectories and evolution of wave characteristics along the rays. Absorption along the rays is calculated by using Poynting's theorem, where local wave dissipation is expressed in terms of the anti-Hermitian part of the hot dielectric tensor. In addition, hot electron and ion correction terms are included in the electric field polarization factors in the absorption calculations. Absorption mechanisms include electron Landau and TTMP, ion cyclotron resonances at the fundamental and higher harmonics for thermal and slowing down distributions. At present, beam energetic ion absorption is modeled by an equivalent Maxwellian distribution with a characteristic temperature and anisotropy.

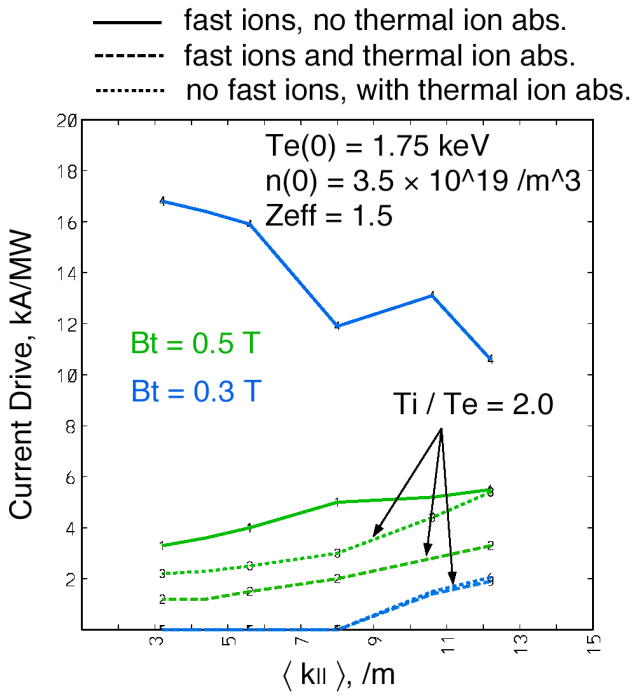

Figure 2. HHFW current drive for various antenna phasings, given as a weighted parallel wavenumber, in the presence of beam fast ions and with and without thermal ion absorption.

Some ideal MHD analysis will be given for selected scenario flattop plasmas. These are analyzed using an equilibrium description directly from TSC, which is read into the fixed boundary equilibrium code JSOLVER. JSOLVER recalculates the equilibrium with high resolution for stability analysis. High-n ballooning stability is calculated with BALMSC, and n=1 external kink stability is done with PEST2 and VACUUM. By now it is well known that low aspect ratio plasmas require significant computational resolution, particularly for kink analysis, and the ideal MHD assessments made here are continuing.

Overall the integrated scenario modeling effort on NSTX will evolve with progress in physics and computations that meet the needs of low aspect ratio exploration. The integrated scenario modeling for

NSTX will greatly benefit from the SciDAC supported numerical simulation of fundamental plasma processes, the continued expansion of the NTCC (National Transport Code Collaboratory) collection of portable physics modules, and the recent Advanced Computing Integrated Simulation Initiative to support integrated modeling code development in fusion sciences.

4.4 100% Non-inductive Discharge Simulations

The discharge simulations to produce 100% non-inductive current, an intermediate goal of the five year plan, were extensions of a particular shot 109070, which was a NBI heated discharge where a sufficiently long pulse had been obtained, the non-inductive current fraction was already about 50%, and high β_N and HH values were reached. The 100% non-inductive goal is being sought by utilizing the following; 1) injection of 6.0 MW of HHFW and 3.0 MW of EBW in addition to the approximately 5.0 MW of NBI power to raise the plasma stored energy, 2) controlling plasma density to enhance the external CD from the HHFW and EBW and/or NBI, and 3) increasing the plasma elongation to increase the safety factor, which increases the bootstrap current contribution. From global theory, the

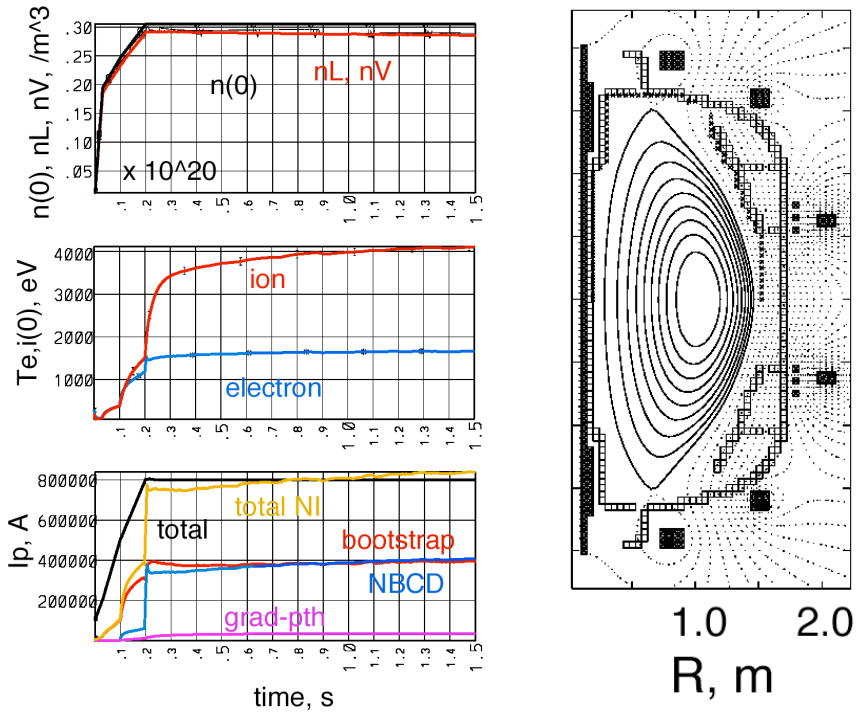

Figure 3. Time histories of β_N, peak temperatures, density, and contributions to the plasma current for the NBI + HHFW simulation to obtain 100% non-inductive current.

bootstrap current fraction is proportional to $C_{BS}\beta_N q_{cyl}$, where C_{BS} contains profile and collisionality effects, and q_{cyl} is given by $\pi a^2 B_t(1+\kappa^2)/\mu_o R I_P$. The bootstrap contribution is enhanced by the increase in plasma stored energy through β_N and elongation through q_{cyl}. These scenarios are done at a toroidal field of 0.5 T to keep q_{cyl} high for bootstrap current. This means that a maximum pulse length of 1.5 s is available. Peaking of the plasma density profile would also enhance the bootstrap current, and this documents present plans for pumping and pellet injection to control the density profile.

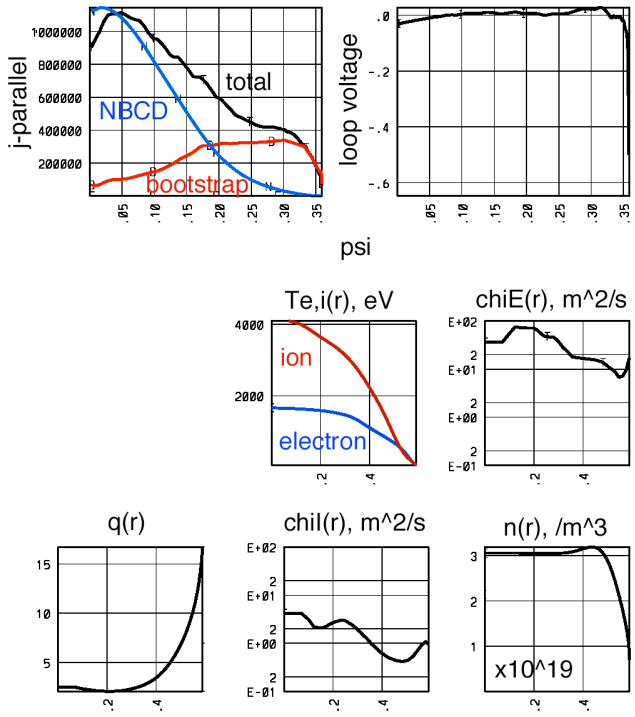

Figure 4. Profiles of temperature, density, safety factor, and parallel current density, and the poloidal flux surfaces during the flattop for the NBI+HHFW simulation to obtain 100% non-inductive current.

NBI and HHFW at Lower Density and High Elongation

Analysis with CURRAY of the plasma equilibria from preliminary TSC simulations and beam data supplied from TRANSP analysis of 109070 showed that the amount of current driven by HHFW would be small ($\leq$ 50 kA) over the entire range of $k_{||}$ due to fast ion absorption. Shown in Fig. 2 is the HHFW current drive as a function of $k_{||}$ spectrum with different assumptions for the thermal ion absorption, and toroidal field. Since the predicted currents are low, no CD is assumed from the HHFW, only power, and its profile and split between ions and electrons is determined from the CURRAY calculation. The peak density is lowered from 0.5×10^{20} /m^3 to 0.3×10^{20} /m^3. The NBI power to the plasma is taken as 5 MW (although 6 MW is injected) and 6 MW from HHFW. Shown in Fig. 3 are the plasma current, peak temperatures and densities during the TSC simulation, and in Fig. 4 are shown the plasma profiles during the flattop. Several global parameters are reported in Table 1. The bootstrap current reaches 400 kA, and the NBCD is the also 400 kA. The plasma elongation is 2.6 with a triangularity of just under 0.40. The increased elongation has resulted in

q_{cyl} rising from about 3.2 to 4.4. The total β_N reaches 6.8. The safety factor remains well above 2.0 during the entire discharge due to the broader current profile from the bootstrap current.

	NBI+HHFW	HHFW only	HHFW+EBW	Shot 109070
Ip, kA	800	725	875	800
I_{BS}, kA	395	275	260	240
I_{NBI}, kA	406	0	0	140
I_{HHFW}, kA	0	400	400	0
I_{EBW}, kA	0	0	175	0
$I_{\beta p}$, kA	40	38	40	50
β_t, β_p	**2.6**, 0.38	**2.15**, 0.40	**2.2**, 0.35	2.1, 0.4
q_{cyl}, q_{95}	**4.4**, 10.0	**4.5**, 9.5	**3.8**,8.5	3.3, 10.0
li(1), li(3)	0.60, 0.40	1.05, 0.77	1.0, 0.70	0.67
β_N^{total}, β^{total}	**6.8**, 18.6%	**4.0**, 13.0%	**3.4**, 14.5%	5.9, 16%
W_{total}(kJ)	340	137	165	150
τ_E(ms), τ_{H98}(ms)	22, 16.5	22, 20	17.5, 16.4	34, 27.5
$T_e(0)$, $T_i(0)$, keV	1.7, 4.0	3.5, 2.2	4.0, 2.1	1.1, 1.8
n(0), x10^{20} /m^3	**0.30**	**0.30**	**0.3**	0.5
n(0)/<n>	1.05	**1.50**	1.50	1.05

Table 1. Parameters Obtained for 100% Non-Inductive Plasma Simulations

HHFW Only with Lower Density

For this scenario no NBI is used, so the HHFW can provide significant current to the total plasma current. Analysis with CURRAY showed that varying levels of current could be achieved for different $k_{||}$ spectra. Shown in Fig. 5a and b are plots of the total HHFW driven current as a function of $k_{||}$ with differing assumptions for the peak electron temperature, Z_{eff}, and thermal ion damping using equilibria directly

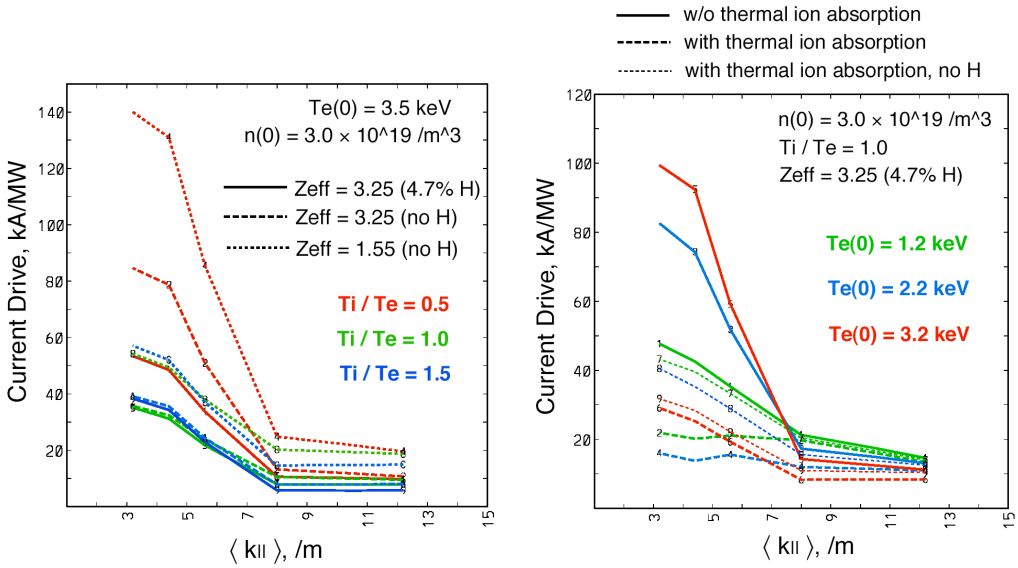

Figure 5 (a). HHFW current drive as a function of antenna phasing, given by a weighted parallel wavenumber, for various assumptions on the ratio of ion to electron temperature and Z_{eff} (b). HHFW current drive for different antenna phasings, given by a weighted parallel wavenumber, for various assumptions of electron temperature and thermal ion damping.

from the TSC simulations. It should be noted that only two passes are allowed for these calculations, that is once the rays reach the outboard plasma boundary where they would reflect, they are stopped. This only affects the lowest temperature cases, leading to reductions in the current drive shown by 1.25-1.7. Otherwise all other cases achieve ≥ 90% absorption. These calculations indicate that the low $k_{||}$ antenna phasings provide the highest current drive efficiency, although this must be balanced against weaker single pass absorption at low temperatures and stronger thermal ion absorption, the net effect still being higher CD efficiency at low $k_{||}$. The impact of impurities and whether the ion temperature is larger or smaller than the electron temperature significantly affects the current drive as well. Shown in Fig. 6 are the current density and electron power density profiles for a HHFW only plasma for a range of launched spectra. These clearly illustrate the central heating and large driven current at low $k_{||}$. The operating

range of electron temperatures in present NSTX discharges and those projected in these scenario calculations indicate complicated behavior for the HHFW current drive, which will need to be verified by theoretical benchmarking and experimental studies. Here the thermal diffusivities and plasma density profile are chosen to match two HHFW only shots, 106194 and 108901. The plasma current is 725 kA in this simulation. The peak density in this scenario is 0.3×10^{20} /m^3, and the total injected power is 6 MW of HHFW. Table 1 shows several parameters for this simulation. The current is composed of 400 kA of HHFW, 275 kA of bootstrap current, and about 38 kA of pressure driven current. In this simulation the elongation could not be raised to enhance the bootstrap current because the li remained high , reaching an elongation around 2.15 and the triangularity about 0.4. The β_N reaches about 4.0. The density profile in this simulation is taken slightly more peaked than those in NBI heated discharges, reflecting the experimental observation.

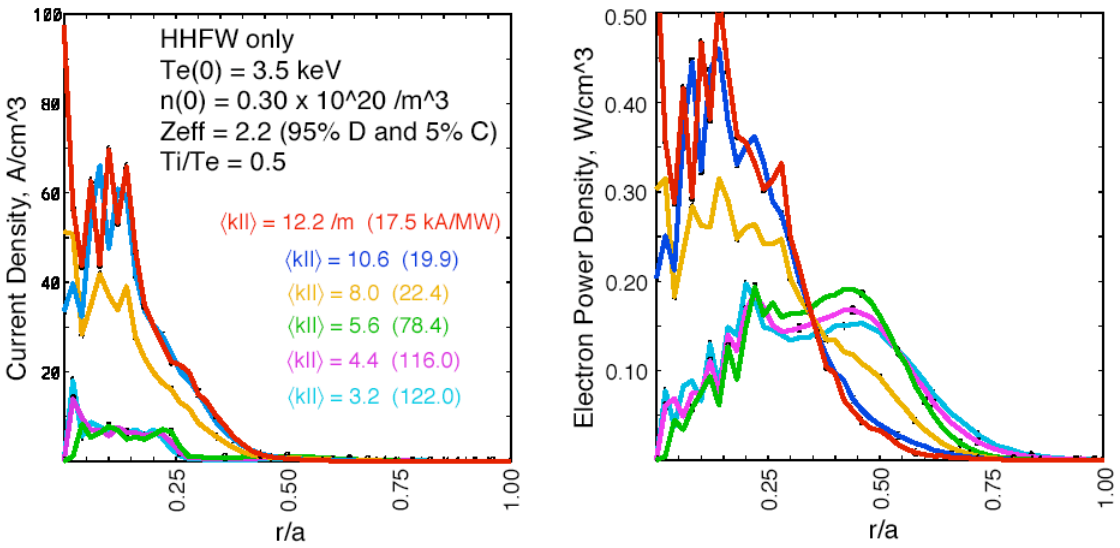

Figure 6. Current density and power density to electrons for a HHFW only case, showing significant current drive under conditions of no NB fast ions and T_i less than T_e.

The scenario can be enhanced by adding EBW heating and current drive, an off-axis source, to increase the stored energy and plasma current. This case is shown in Table 1, with similar plasma shaping. Shown in Fig. 7 is the time history of the plasma current contributions and the peak electron and ion temperatures. Shown in Fig. 8 are various plasma profiles from the simulation. The plasma current reaches 875 kA, with 400 kA of HHFW current, 175 kA of EBW current and 260 kA of bootstrap current.

The safety factor remains above 2.0 throughout the scenario. There is 6 MW of HHFW power and 3.0 MW of EBW power injected.

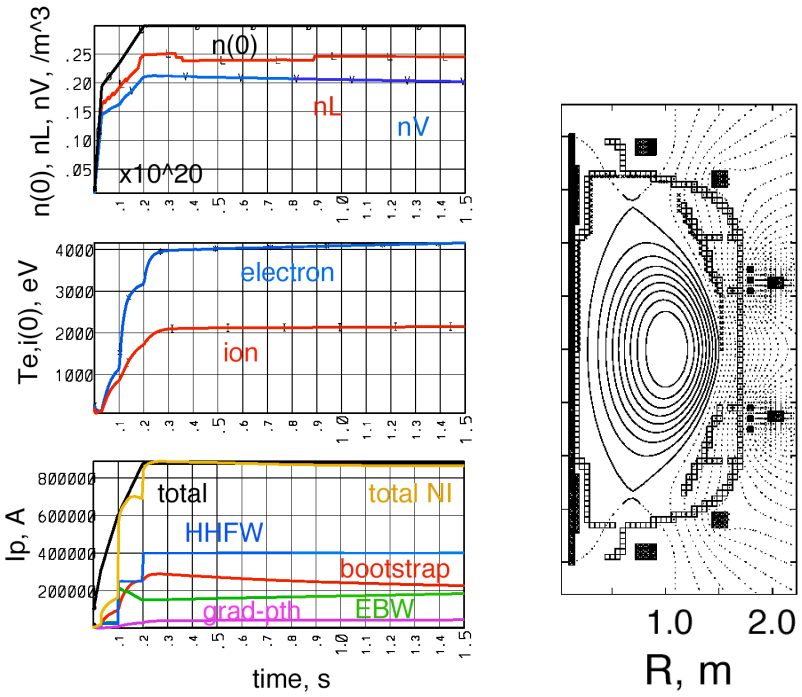

Figure 7. Time histories of β_N, peak temperatures, density, and contributions to the plasma current for the HHFW + EBW simulation to obtain 100% non-inductive current.

The ion energy transport is typically 2-4 times neoclassical, while electron energy transport can range from similar to NBI heated discharges to a factor of 2 lower. The HHFW only discharges do not demonstrate as strong a suppression of ion transport as is seen in NBI heated discharges, leading to ion temperatures that are lower than the electron temperature, greatly improving the CD efficiency of HHFW against thermal ion absorption. The present H-modes produced in HHFW only discharges have higher stored energies, but these are produced by a rising density and a strongly broadened density profile. The electron temperatures did not rise, although pedestals did form. The present simulations have examined the L-mode where high electron temperatures were accessed and RFCD is maximized. H-mode based scenarios will be pursued in the future.

Internal transport barriers have been observed in the electron channel in HHFW only discharges producing more peaked electron temperature and density profiles, although this has not been assumed in these simulations. The addition of such large HHFW power (3 times that in previous experiments), may change some of the transport assumptions, when the experiments are actually performed. A significant

issue uncovered in the analysis is thermal ion absorption by hydrogen and deuterium, which can be strong at lower $k_{||}$, where the CD efficiency is the highest.

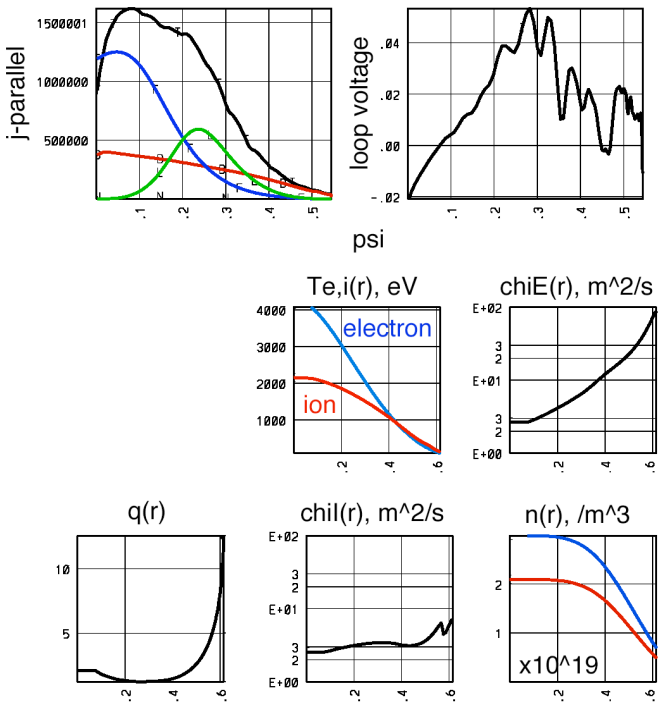

Figure 8. Profiles of temperature, density, safety factor and parallel current density, and poloidal flux surfaces for the HHFW + EBW simulation to obtain 100% non-inductive current.

The 100% non-inductive milestone can be reached in NSTX by utilizing a combination of increased heating, high B_T, high elongation, and lower density ($\sim 0.3 \times 10^{20}$ /m^3). This regime attempts to maximize the bootstrap current. The high B_T restricts the flattop to 1.5 s, which is about 3 current diffusion times for the NBI and HHFW case, and about 1 current diffusion time for the HHFW only cases. Either NBI and HHFW (with little driven current), HHFW only, or HHFW and EBW, at approximately 800 kA, discharges can achieve this goal.

4.5 High β and High β_N Operating Targets

The establishment of the maximum operable plasma pressure is important to identify possible targets for sustainable high β and fully non-inductive operating modes. Initially this exercise is to push to the largest allowable β-limits inside the present experimental device, with copper stabilizer plates and strong plasma rotation, and later with active feedback coils for stabilizing the n=1 RWM. The duration of these plasmas is not important, so that sustainement only over an energy confinement time would be required. In addition, the plasma current is driven inductively. Later, the combination of fully non-inductive (with

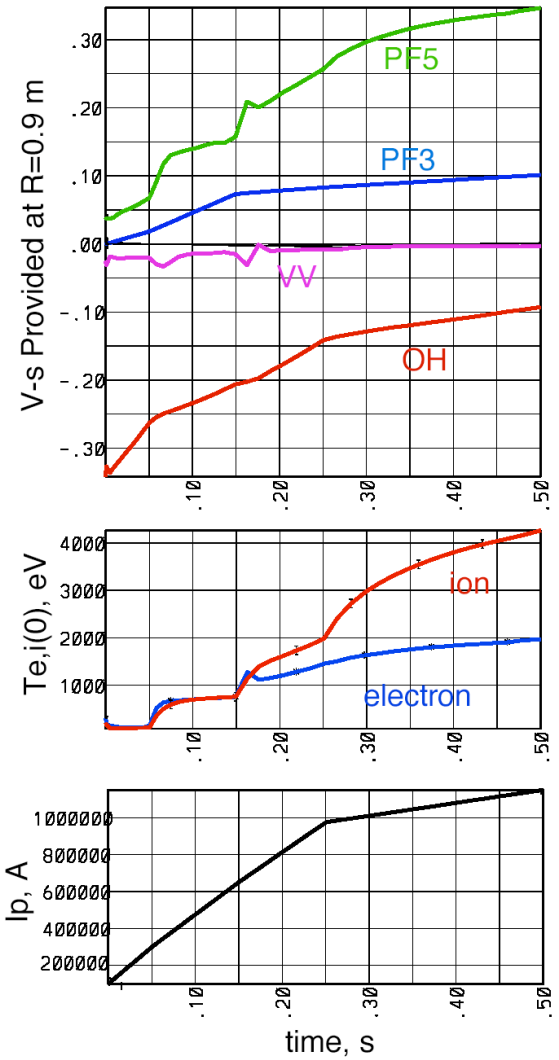

Figure 9. Time histories of the plasma current, peak temperatures and volt-seconds provided by the PF coils to the plasma, and the sequence of plasma boundaries for the high β transient scenario.

high bootstrap fraction) and high β would be sought, with a duration of much greater than a current diffusion time.

Scenario simulations were done to examine accessible β's with inductive current rampup. There are several possible combinations of density, current, heating, and plasma shaping evolutions to produce different pressure and current profiles. Here the plasma current was ramped up to 975 kA in 0.25 s, and then up to 1.15 MA in 0.5 s. The heating consisted of 5 MW of NBI and 6.0 MW of HHFW, both centrally deposited. The plasma density is ramped up to 0.3 $\times 10^{20}$ /m^3 in 0.25 s and held fixed at that value. The power is injected in three steps 3 MW of HHFW at 0.05 s, 2 MW of NBI and 6 MW of HHFW at 0.15 s and then 5 MW of NBI and 6 MW of HHFW at 0.25 s. Shown in Figure 9 are time trajectories of several parameters. Included in Figure 10 are the profile time histories for the toroidal current density, plasma pressure, and loop voltage, as well as a sequence of plasma boundaries as the plasma is grown.

The plasma obtains a β of 46%, with β_N of 8.4. The plasma current is 1.15 MA, which corresponds to a time of 0.5 s. The toroidal field was 0.365 T. The plasma elongation was 2.6 with a triangularity of 0.7, which is accessible with a modification to PF1. This plasma was stable to high-n ballooning and n=1 kink mode with a wall on the outboard only at 1.5a measured from the plasma center. It is clear that access to transient high β plasma configurations are

possible, as already demonstrated in NSTX, which will allow a careful verification of MHD theory in the low aspect ratio regime. Shown in Fig. 11 are several equilibrium profiles for this plasma, as well as the poloidal flux surfaces at 46% toroidal beta.

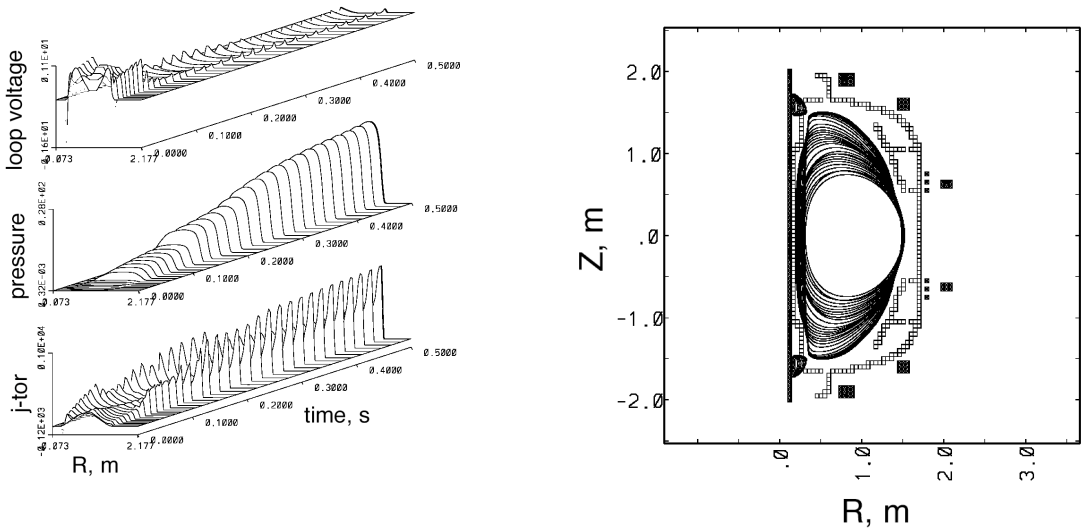

Figure 10. Profile time histories for the toroidal current density, plasma pressure, and loop voltage, as well as a sequence of plasma boundaries, for the transient high β scenario.

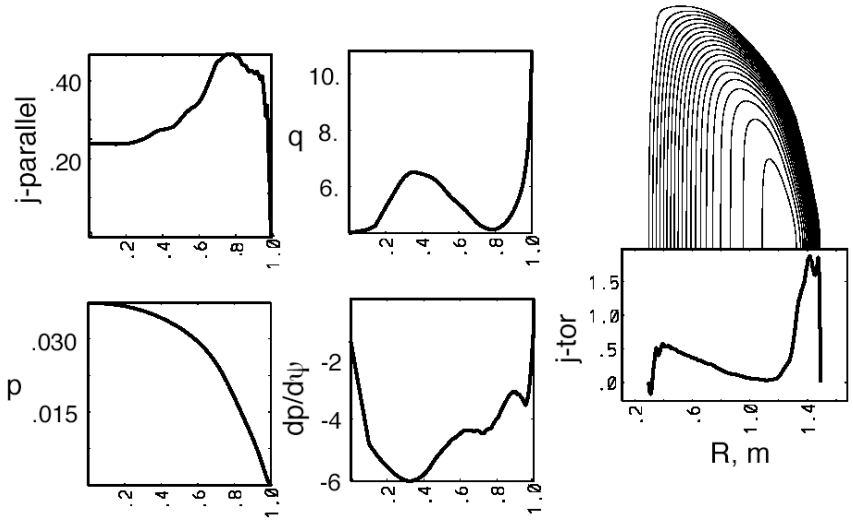

Figure 11. The transient high β = 46% equilibrium profiles vs. √V/Vo, and poloidal flux surfaces, showing the strong plasma shaping, beam pressure gradient in the core, strong off-axis current density, and strong Shafranov shift of flux surfaces.

4.6 No-OH Coil Initiation and Current Rampup

The no-OH Coil initiation and current rampup is considered a critical goal of the ST program since its attractiveness is directly tied to eliminating the OH solenoid on the inboard side of the device and allowing access to compact geometry. This milestone can be divided into 3 primary thrusts; 1) initiation with outer PF coils, and or Coaxial Helicity Injection, 2) low density rampup phase typically achieved with an RF source due to limitations on NBI, and 3) the high density rampup phase which would include the use of NBI to end up at an attractive advanced plasma configuration. The time-scales required for this type of rampup (current diffusion times) are long compared to those required with inductive current rampup due to the reliance on bootstrap current, which is an off-axis source of current, and the hollowing effect of the current profile that results from off-axis current drive. The external HHFW (on-axis) , EBW (off-axis), and NB (on-axis) current drive would also be present. The formation of a "current hole" might allow faster ramps if it is stable, however, one ultimately wants this configuration to relax and fill the current hole back in. For the present simulations current holes are avoided, which should set the longest time scales required for such a discharge. The available flattop is determined by the toroidal field, 1.5 s for 0.5 T and 5.0 s for 0.3 T, for example.

The simulations assume that the plasma starts the rampup at 100 kA, provided by the initiation and early ramp phase, which is treated as inductive current. HHFW is the current drive source in the low density phase, and NBI is added in the high density phase. EBW can also be applied in these current rampup phases, but has not been examined here. The toroidal field is 0.45 T, to enhance the bootstrap current through q_{95}, although it limits the pulse length available. Shown in Fig. 12 are the plasma current, peak temperature, density, and β_p and l_i as a function of time, and in Fig. 13 are plasma profiles at t=2.0 s. The simulation is run out to 4 s, beyond the TF coil flattop to show how the plasma would further relax.

In the low density phase the HHFW power is ramped slowly to avoid current hole formation, while the density is ramped to keep the temperature sufficiently low to access short current diffusion time-scales. In order to keep the temperature from increasing too fast in this phase the plasma is limited to avoid transition to H-mode. The peak electron temperature reaches 1.3 keV, while the density ramps up to 0.3×10^{20} /m^3 over 0.3 s. The poloidal β reaches 3.0 in this phase since the total plasma current is low. Around 0.3-0.4 s the plasma is diverted, allowing an improvement in global confinement, with the poloidal β reaching 4.0. Then beginning at 0.5s the NBI power is stepped up in 2.0 MW increments,

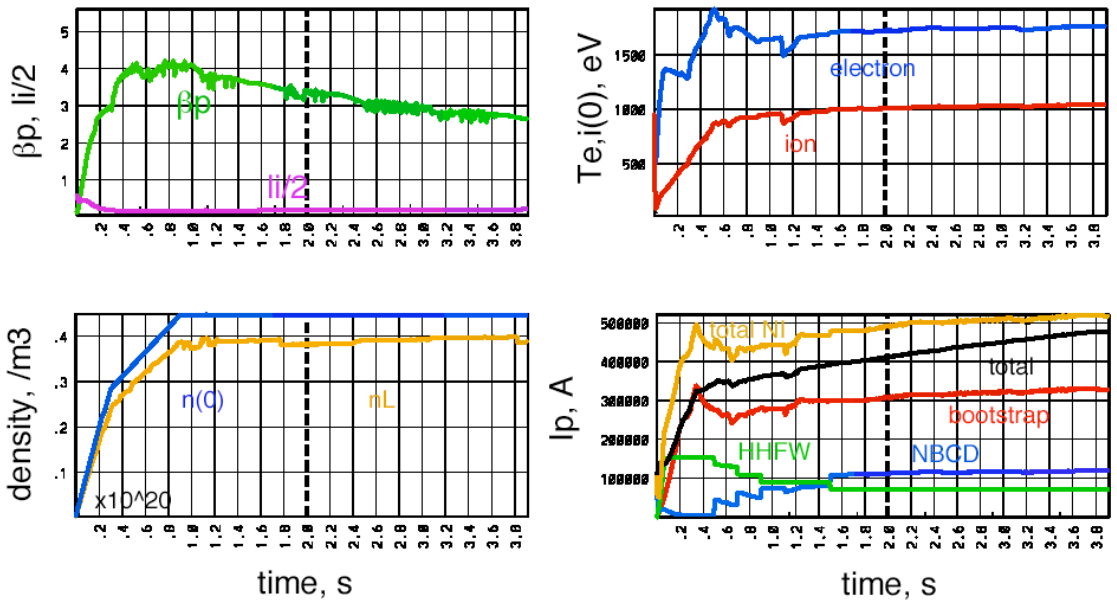

Figure 12. Time histories of the βp and li, temperatures, density, and contributions to the plasma current for the no-OH Coil current rampup simulation.

although lower powers are assumed because the total plasma current is too low to fully confine the beam particles. The corresponding total NB driven current is about 50 kA, 75 kA, and 110 kA, based on the beam confinement observed in experimental rampups, where NBI is turned on at currents below 800 kA. The heating and driven current from the

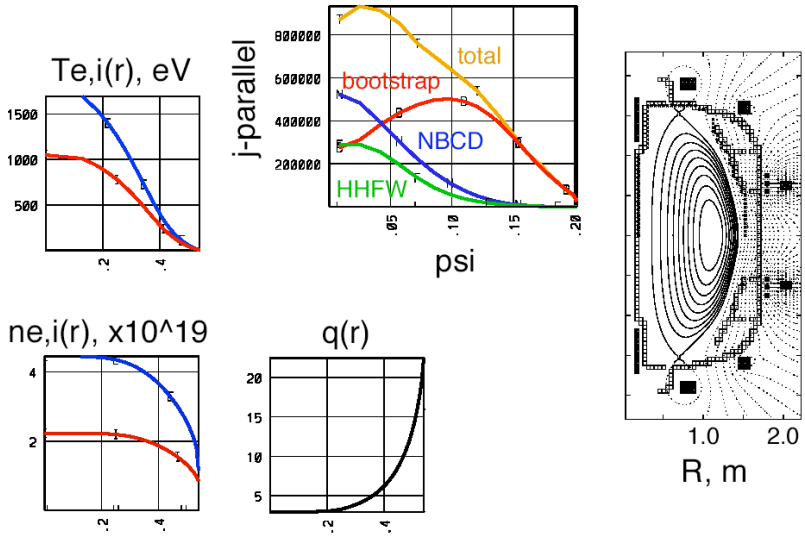

Figure 13. Profiles of the temperatures, densities, safety factor, and parallel current density, and poloidal flux surfaces for the no-OH Coil current rampup simulation.

beam would continue to improve as the plasma current increased. In addition, the poloidal β drops reaching 2.75 by 4.0 s. The β_N reaches about 5.5 during discharge simulation and relaxes to 5.0 by 4 s. By 2 s the total plasma current has reached just over 400 kA, and by 4 s has reached almost 500 kA. The HHFW current begins to drop after 0.5 s due to the rising density and onset of NBI which would provide fast ions to absorb the FW power. Since the beam is not well confined over this simulation the HHFW current is expected to persist. From NSTX discharges NBI is always initiated at low currents (below 800 kA). Based on the TRANSP analysis for shot 109070 the fraction of beam power absorbed at a given plasma current is used here to scale the power absorbed in the plasma and the fast ion density, which is used to estimate the HHFW current drive. Shown in Figure 14 are the contributions of the various PF coils to the volt-seconds during the rampup, and the total flux state as a function of time.

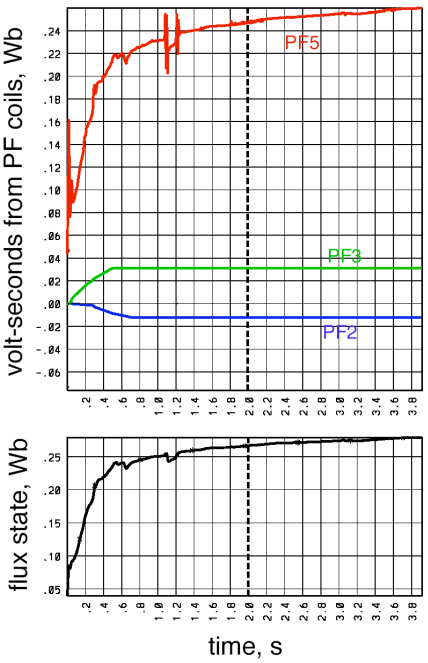

Figure 14. Contributions of the PF Coils to the volt-seconds during the no-OH current rampup simulation.

Another simulation was performed in which only heating from the HHFW was assumed, which causes the bootstrap current to be the only current drive source, apart from the assistance provided by the PF coils. The plasma current ramped up to approximately 275 kA by 0.5 s, compared to about 350 kA with HHFW CD. The current profile was quite broad, since only bootstrap current is driven non-indcutively, with li(1) reaching 0.4, li(3) reaching 0.2, and β_p obtaining 5.6. It was very difficult in the simulation to control the plasma shape which became highly elongated reaching 3.5. This can be another method for producing no-OH current rampup, which would certainly be more susceptible to current hole formation. This does demonstrate the strong coupling of plasma shaping and current profile at low li and will be critical to controlling the discharge evolution for these types of plasmas.

The simulations of the no-OH current rampup demonstrate that the feasibility of such a procedure is consistent with 1.5D modeling, and in light of experimental demonstrations on JT-60U of such a rampup with Lower Hybrid and NBI, there is some confidence that this can be achieved in NSTX. Establishing the plasma transport and operational behavior of this regime in the experiment will greatly enhance the modeling of the rampup procedure.

4.7 Fully Non-inductive High β Scenarios for Longer Than a Current Diffusion Time

Ultimately, the fully non-inductive and high β features of earlier discharge scenarios must be combined to produce an attractive plasma configuration that can be projected to steady state and high fusion performance. The features necessary to demonstrate this are 1) 100% non-inductive current which maximizes the bootstrap current fraction, 2) high β that is sustainable, and 3) a quasi-stationary state with a duration much longer than a current diffusion time. Since the heating is provided by NBI , HHFW and EBW the current will be composed of NB driven, EBW and bootstrap current, the fast ion absorption making the HHFW driven current very low. It is desired to maximize the bootstrap current fraction, and so the elongation is maximized and the lower plasma currents are used. However, the actual bootstrap current achievable will also depend on the accessible β_N, which is determined by the toroidal field, energy confinement, and MHD stability. Since these plasmas must have flattop times longer than a current diffusion time, a lower toroidal field is desired, providing up to 5 s pulse lengths at 0.3 T.

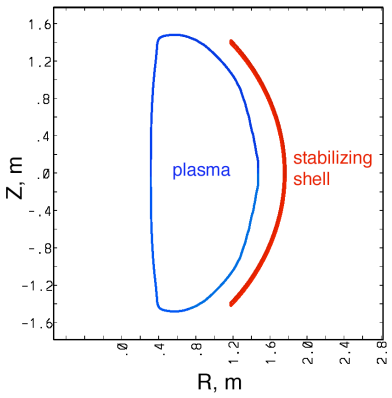

Figure 15. Fully non-inductive high β plasma 99.5% flux surface and ideal conducting wall used in n=1 kink stability analysis.

An attractive configuration was found which is stable to high-n ballooning and the n=1 kink mode, with a simple outboard wall located at 1.5a. This is shown in Figure 15, and represents a conservative estimate of the wall stabilization for n=1. Further analysis is required to assess high toroidal mode numbers. The

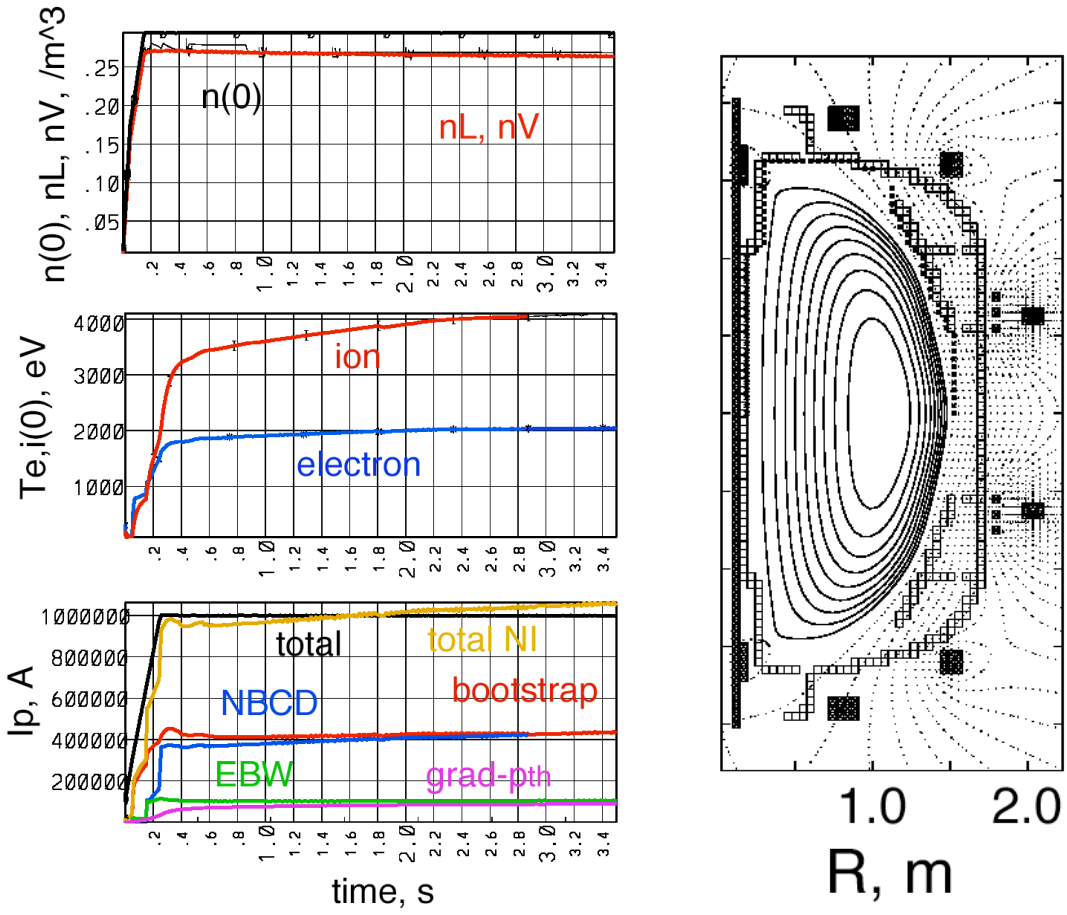

Figure 16. Time histories of the plasma density, temperature and contributions to the plasma current during a simulation of the fully non-inductive high scenario with TSC.

ideal MHD stability played a critical role in constraining the space of viable configurations, particularly since the available auxiliary power on NSTX is larger than required to reach high stored energy. The plasma has strong shaping accessible with a modification of PF1, allowing elongation up to 2.6 combined with a triangularity of 0.6. Without this modification the shapes would be limited to =2.8, =0.4 or =2.0, =0.8, with some limited number of intermediate shapes from single null operation. In addition, the use of EBW for off-axis bulk current drive was required to augment the bootstrap current to

reach broad current profiles at higher plasma current. Analysis indicated that for the high β plasmas of interest at a peak density of 0.35 $\times 10^{20}$ /m^3 and peak temperature of 1. 5 keV, a CD efficiency of 35 kA/MW could be achieved fairly uniformly between normalized minor radii of 0.4 to 0.7. The CD for EBW used in the simulation scales this result as the ratio T_e/n. Shown in Figure 16 are the temperature, density, and plasma current time histories from the simulation for the 3.5 s pulse to the end of flattop. Also shown are the poloidal flux contours. Shown in Figure 17 are the profiles of parallel current, loop voltage, temperatures, density, and safety factor.

The plasma current is ramped up to 1.0 MA in 0.25 s and the toroidal field is 0.365 T. Approximately 0.64 V-s are linked by the plasma, however, only 0.25 V-s are from the OH coil, 0.31 V-s are from PF5 and 0.08 V-s are from PF3. The total injected power is 10 MW, composed of 4 MW of NBI centrally deposited, 3 MW of HHFW centrally deposited, and 3 MW of EBW deposited at a normalized minor radius of 0.65. The peak density reaches 3.0 $\times 10^{20}$ /m^3 and the peak temperatures are 4.0 keV for ions and 2.0 keV for electrons. The plasma major radius is 0.89 m, minor radius is 0.59 m, elongation is 2.55 and triangularity is 0.63. The β flattops at 41.3% and β_N is 8.85, with β_p of 1.6. The safety factor is above 3.0 everywhere, and has a reversed shear region inside of r/a=0.7. The plasma stored energy reaches 442 kJ, and the energy confinement time is 37 ms, which is 1.5 times IPB98(y,2) scaling. The bootstrap current is 430 kA, the beam driven current is 430 kA, EBW current is 100 kA, and the β_p

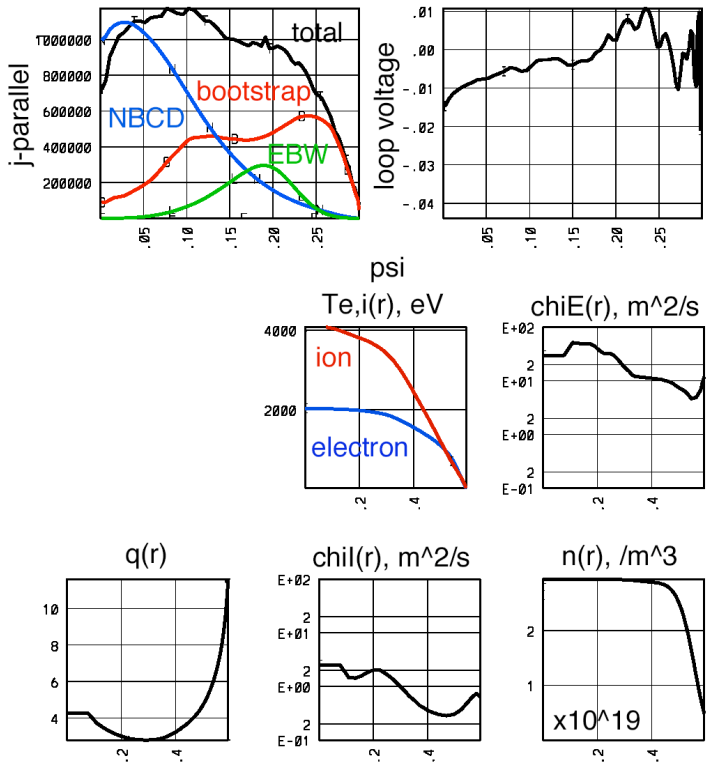

Figure 17. Profiles of the parallel current, loop voltage, temperatures, density, safety factor and thermal diffusivities from the simulation of the fully non-inductive high β scenario with TSC.

current is 88 kA, giving very slight overdrive at the end of the flattop. The current profile is broad with li(1) at 0.4 and li(3) at 0.25. The current diffusion time for this plasma is about 750 ms, while the flattop time is about 3.0 s, allowing for 4 current diffusion times.

4.8 Investigations and Development for Integrated Scenario Modeling

The improvement of modeling is a continuous process, both based on experimental observations and progress in theoretical/computational capability. From the simulations done so far, to examine the access to high performance plasmas in NSTX, a number of issues have been identified that require better definition, and these are briefly discussed below.

Non-Inductive Current Contributions

Apart from the external sources of non-inductive current, NBCD and HHFW CD, are the bootstrap current, the Pfirsch-Schluter (PS) and diamagnetic currents, often referred to as self-driven currents. It is important to determine these currents to be able to assess the approach to zero loop voltage, or 100% non-inductive current. Effects on the bootstrap current due to distortions in the thermal ion and electron distribution functions associated with neutral beam and RF heating need to be calculated and included.

HHFW Current Drive Efficiency

The HHFW current drive in NSTX has demonstrated excellent results in initial discharges with 2 MW of power, both in heating electrons and driving current levels similar to those calculated. However, it has also been identified both theoretically and experimentally that fast ions from the beams will absorb significant fractions of the power and ultimately reduce the current drive significantly. In fact, due to this projection, the driven current from HHFW was ignored in simulations that combine HHFW and NBI. In experiments with NBI and HHFW, lower toroidal field showed a weaker fast ion absorption than at high toroidal field. Analysis with CURRAY indicates that higher electron temperatures or densities can reduce the fast ion absorption. The actual impact is likely to depend sensitively on discharge parameters, and so this will likely require experimental verification. In addition, improved modeling using Fokker-Planck

derived distribution functions for the fast ions rather than high temperature Maxwellians or model slowing down distributions is necessary.

Analysis of HHFW with the CURRAY and HPRT ray-tracing codes, has found a discrepancy in the thermal ion absorption, with CURRAY predicting larger absorption. This issue is important to resolve since it would affect the HHFW only discharges, again reducing the power absorbed on electrons and the resulting current drive. Simulations with AORSA (full-wave), gives a thermal ion absorption that is roughly in between the two ray-tracing codes. This issue appears most prominently at low $k_{||}$, which has weaker single-pass absorption, aggravating the ion absorption, although this is the $k_{||}$ required for significant current drive. Part of this issue depends on knowledge of the impurity species present in the device, with hydrogen being the most effective as a thermal ion absorber. Efforts to reduce the impurities and better characterize the species mixture will be incorporated into simulations as they develop. To date the evidence for thermal ion absorption of HHFWs in the experiment are absent.

The benchmarking of ray-tracing and full wave analysis for HHFW is an ongoing exercise, and will likely be used to address the issues outlined above as well. Up to now the comparisons have shown the two approaches to be in agreement, which is expected based on the properties of the fast wave. The full wave analysis is much more computational intensive than ray-tracing, and so ray-tracing will likely remain the primary tool for scenario modeling, particularly when integrating with/into transport codes like TRANSP and TSC. Ultimately, this will provide a lookup table for use in TSC or TRANSP dynamic evolutions where the plasma parameters vary significantly over the discharge. Efforts are also underway to integrate CURRAY into TRANSP.

Electron Bernstein Wave Current Drive

The assessment of EBW current drive is in its early stages and projections based on this technique are preliminary. However, the CD efficiencies and accessibility in plasma radius are promising. This technique has significant potential in the areas of bulk current drive, NTM stabilization, and transport control, as demonstrated with ECCD on various tokamaks. The scenario modeling shows that the fully non-inductive high configurations depend strongly on obtaining off-axis current to maintain high

current and a broad current profile for ideal MHD stability. Its continued progress will be incorporated in the scenario modeling.

NBI Analysis

Neutral beam injection is a source of heating, current drive, and rotation in NSTX, and is considered a central component to future ST devices. The Monte Carlo treatment in TRANSP is considered very good even at low aspect ratios. For NSTX no-OH Coil advanced scenarios, the beam confinement at low plasma current is of particular interest. In NSTX discharges the NBI is typically injected during the current rampup at lower plasma currents, and the lack of total confinement is clear from TRANSP analysis of absorbed power in every NBI heated discharge. A plasma current of approximately 800 kA is considered the level where beam confinement is high, although orbit losses can still account for 5-15% loss of the beam energy depending on the plasma proximity to the outboard structures. It should be noted that different discharge parameters can change this somewhat. In the no-OH Coil simulation the neutral beam is injected when the plasma current is only 350 kA, and significant beam losses are expected. The plasmas produced during this scenario are also very high β_p which should also affect beam confinement. All the simulations presented here used the beam parameters from shot 109070, so that more consistent beam analysis is required in future analysis.

In addition, increasing the beam energy, from 80 to 100 keV, may be necessary to increase the beam power for pushing β-limits in the high β scenarios. Previous experiments did not show increased losses at the higher energy, however, the high β and high β_N plasma configurations should be examined to verify beam confinement.

Plasma Transport

Although many simulations involve constraining the transport coefficients to those of a particular experimental shot, both TRANSP and TSC have the GLF23 and MMM95, as well as L-mode and neoclassical, theory based transport models available, which are widely used in predicting tokamak behavior. Their applicability to NSTX at low aspect ratio is of particular interest and will be pursued. Further diagnosis of the experimental thermal and particle diffusivities is also required, in particular, what

are is the relative confinement in the ion and electron channels when equal amounts of NBI and HHFW are injected, versus their values when only NBI or only HHFW are injected. The global scaling of the confinement in various regimes with plasma current, toroidal field, auxiliary power, etc. are needed in scenario modeling to better project the thermal diffusivities into discharges not yet produced.

The impurities are important in properly understanding the particle species and their balance in NSTX, as well as its effects on NB and HHFW current drive, radiated power, thermal transport, and bootstrap current. Improved coupling of this experimental information into scenarios will continue.

Density Evolution

The density evolution in the scenario modeling has assumed that flattops can be obtained where the density is held at a desired value for the plasma current flattop time. Presently this is not possible in NSTX, but near term device upgrades are intended to address density control. This is critical for current drive from NBI, HHFW and EBW, but also provides significant flexibility to the experiment to produce high performance discharges under varying conditions in plasma transport, injected power, toroidal field, and plasma current.

MHD Stability

The scenario simulations using TSC have shown that high β_N and high β discharges should be energetically accessible with NBI, HHFW and EBW heating, based on thermal diffusivities from existing discharges. Ideal MHD stability analysis of several of these scenario plasmas indicates that high-n ballooning instability typically sets the lower limit on β_N, while the n=1 external kink mode could obtain the higher β_N values. The proposed modification of the PF1 coil has allowed access to a combination of high elongation and high triangularity, which are only accessible separately without the modification. The improvement in the ballooning stability is very significant and easily seen in analysis of a number of scenario equilibria. The actual limits reached in the experiment will be determined by a number of complicating features which have not been included in present analysis, but will be pursued ; 1) the actual conductor geometry with close by copper stabilizers off the midplane and a steel vacuum vessel that is further away at the midplane, 2) plasma rotation speeds approaching 20% of the Alfven speed, 3) possibility of higher n external kink modes providing lower limits than n=1, 4) neoclassical tearing modes

appearing at lower pressures, 5) effects of feedback stabilization with active coils, 6) success in obtaining the plasma shapes identified in these scenarios or others with higher triangularity, and 7) how high-n ballooning modes will limit the pressure, since they are not observed to produce disruptions experimentally, and should "adjust" the local pressure gradients to be marginal. The analysis tools and approximation of the actual experimental situation will be improving over this 5 year period, allowing for better predictions of accessibility to high pressure plasmas.